International Journal of Scientific Research in Engineering and Management (IJSREM)
Volume: 10 Issue: 10 | Oct - 2026 SJIF Rating: 8.659 ISSN: 2582-3930

Enhancement of Microgrid Efficiency through Strategic Management of Distributed Energy Resources Integrated Unified Power Quality Conditioner

Routhu Soujanya[1] Manugonda Pakkiranna[2], Rambabu.Yerra[3], T. Rajeswari[4]

[1]Electrical and Electronics Engineering & Holy Mary Institute of Technology and Science
[2]Electrical and Electronics Engineering & Holy Mary Institute of Technology and Science
[3]Electrical and Electronics Engineering & Holy Mary Institute of Technology and Science
[4]Electrical and Electronics Engineering & Holy Mary Institute of Technology and Science

---

Abstract—Low-voltage microgrids incorporating photovoltaic (PV) generation face intermittent power injection, nonlinear-load harmonics, voltage disturbances and converter overcurrent. This paper consolidates a coordinated photovoltaic–battery energy storage system (BESS)–unified power quality conditioner (UPQC) architecture for simultaneous energy management and power-quality compensation. A series converter regulates the load-side voltage, while a shunt converter suppresses current harmonics, supplies reactive current and controls the common DC link. A bidirectional battery converter uses a state-of-charge-aware dynamic power reference, and adaptive current-sharing factors protect the shunt converter during excessive load transients. Results reported in the source documentation include a reduction of grid-current total harmonic distortion from a 27.61% nonlinear-load current to 2.47% in a normal operating case, while protection mode permits a temporary 7.70% grid-current THD to avoid overloading the converter. The paper examines system design, controller logic, representative waveforms, operating constraints and validation limitations.

Index Terms—Microgrid, UPQC, photovoltaic generation, battery storage, power quality, total harmonic distortion, current limiting.

I. INTRODUCTION

Distributed energy resources improve the flexibility of distribution networks, but converter-rich microgrids are sensitive to harmonics, voltage sag, reactive power demand and variable renewable generation. A unified power quality conditioner combines a series voltage-source converter (SeC) and a parallel/shunt converter (PaC) through a common DC-link capacitor. The SeC injects compensating voltage to protect sensitive loads; the PaC shapes grid current and balances the DC-link energy.

In the studied arrangement, the PV array is coupled to the common DC link, whereas the battery connects through a bidirectional DC–DC converter. This architecture supports PV utilization, charging/discharging coordination and power-quality correction. Its principal limitation is the finite current rating of semiconductor switches during uncertain load surges. The source work therefore introduces a current-component-aware protection mechanism.

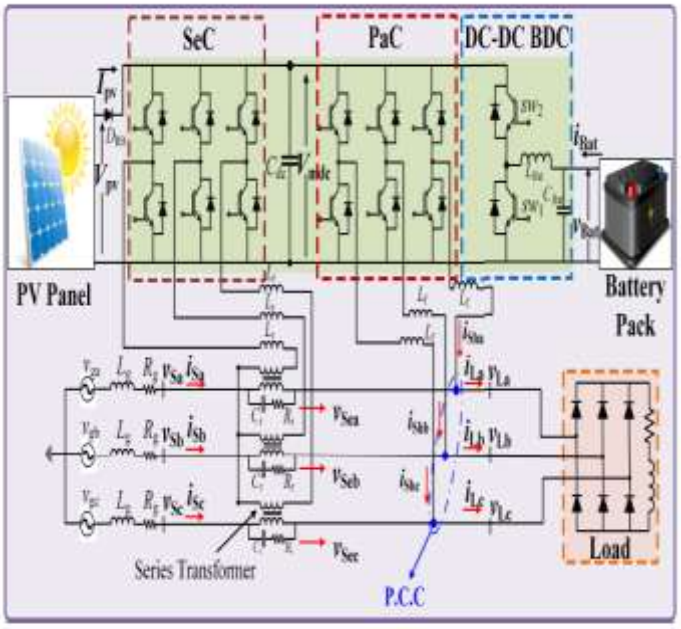


Fig. 1. PV–BESS–UPQC microgrid power-stage architecture (reproduced from supplied documentation).

II. RELATED WORK AND RESEARCH MOTIVATION

The supplied review discusses grid-following and grid-forming DER inverters, multi-objective UPQC interfaces, hydro-generator UPQC systems, feed-forward DC-link regulation and sequence-based fault-current limitation. The common challenge is to coordinate current quality, voltage support and DER power sharing without sacrificing converter protection. Battery-supported UPQC designs additionally need to handle battery state-of-charge constraints.

Compared with purely passive or hardware current limiting, the documented method modifies reference current components in the controller. This permits temporary redistribution of harmonic and reactive current to the grid when the converter reaches its limits. Such a trade-off must be distinguished from permanent compliance with harmonic limits.

III. SYSTEM CONFIGURATION AND POWER BALANCE

The studied system comprises a three-phase grid, a nonlinear diode-rectifier load, series injection transformers, a shunt voltage-source converter, a common DC capacitor, PV

modules and a bidirectional battery converter. The nominal line-to-line AC voltage reported in the documentation is 110 V rms and the nominal DC-link operating voltage is 200 V. The source considers substantial grid-voltage sag capability and converter sizing based on harmonic, reactive and active power contributions.

Ignoring conversion losses, the approximate active-power balance can be written as $P_{grid} + P_{PV} + P_{BESS} = P_{load} + dE_{DC}/dt$. With $E_{DC} = (1/2)C_{DC} V_{DC}^2$, a disturbance in generation or demand appears as a DC-link voltage deviation until the shunt controller and BESS respond. The sign convention for charging and discharging must be implemented consistently in both the battery and grid-current reference blocks.

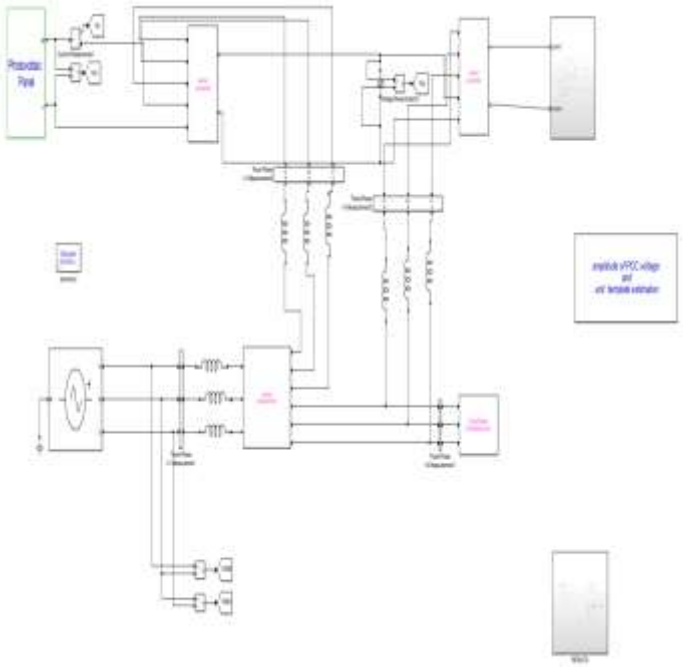


Fig. 2. MATLAB/Simulink system-level implementation shown in the supplied source.

The PV maximum-power-point tracking reference is constrained by the converter's safe DC-link voltage range. The battery converter is operated in current control using a dynamic power request rather than being assigned sole responsibility for DC-link regulation.

IV. COORDINATED CONTROL DESIGN

A normalized comb filter and second-order harmonic oscillator estimator are used in the source to obtain fundamental positive-sequence voltage templates. A modified inverse notch filter extracts fundamental load-current information. The load current is decomposed into active, quadrature/reactive and harmonic components, enabling selective compensation and current limitation.

The shunt-converter reference includes the fundamental active load component, the DC-link regulation current and PV/BESS feed-forward currents. A hysteresis current controller then generates the shunt-converter gating pulses. The series converter forms a reference injection voltage from the difference between the desired sinusoidal load voltage and the measured grid voltage.

The DC-link controller uses a proportional–integral (PI) law, with source-reported gains $K_p = 1$ and $K_i = 10$. The battery-current controller employs source-reported $K_{p,B} = 0.45$ and $K_{i,B} = 9$. The reference battery current is determined from the battery power request divided by battery terminal voltage, subject to SOC and converter constraints.

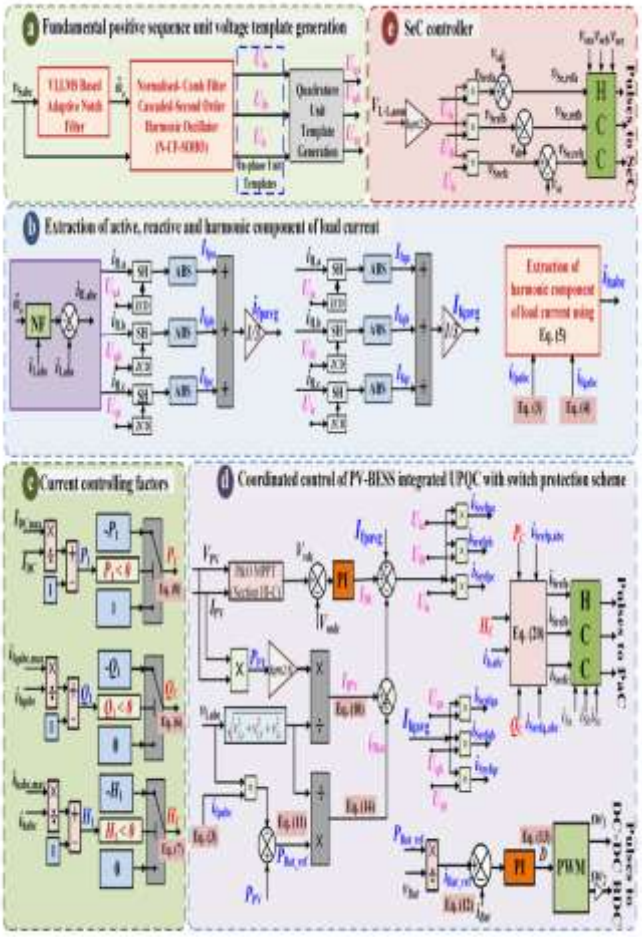


Fig. 3. Coordinated control and switch-protection block diagram (source figure).

V. SWITCH PROTECTION AND STABILITY

A shunt converter must supply harmonic and reactive compensation current as well as DC-link regulation current. Sudden load increases may cause the sum of these components to exceed the safe switch-current envelope. The documented algorithm applies protection factors to harmonic, reactive and DC-link components and redirects excess demand to the grid during the transient. This approach preserves semiconductor safety at the expense of temporary deterioration in grid-current quality.

The reported current-limiting action occurs within one fundamental cycle following the transient. The documented protection case is activated at approximately $t = 0.25$ s. The DC-link regulation component remains within its permissible range in that case, whereas harmonic and reactive components trigger their respective protection factors.

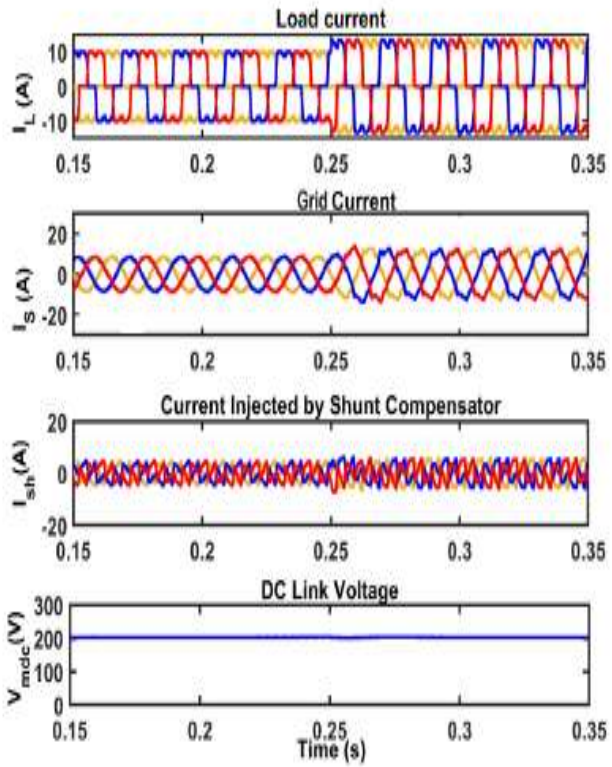


Fig. 4. Load, grid and compensator current waveforms with DC-link voltage during switch protection.

Small-signal analysis of the DC-link loop relates capacitor current to the DC-link voltage derivative. The supplied documentation reports a compensated-loop phase margin of approximately 86° at 144 rad/s using the stated PI gains. This is a source-reported analytical result; a fresh frequency-domain calculation requires the complete plant parameters and controller implementation.

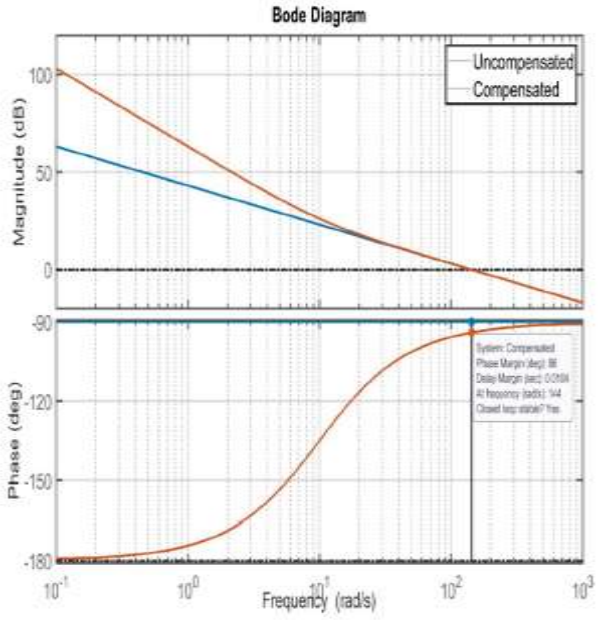


Fig. 5. Source-reported frequency response of the DC-link control loop.

VI. SIMULATION RESULTS: NORMAL OPERATING CONDITIONS

The source evaluates the proposed arrangement in MATLAB/Simulink under nonlinear loading, changes in PV power and battery SOC, and power-quality disturbances. At an irradiance of 1000 W/m², the shunt converter compensates distorted load current so that the grid current approaches a balanced sinusoidal waveform. The reported load-current THD is 27.61%, compared with 2.47% for the compensated grid current.

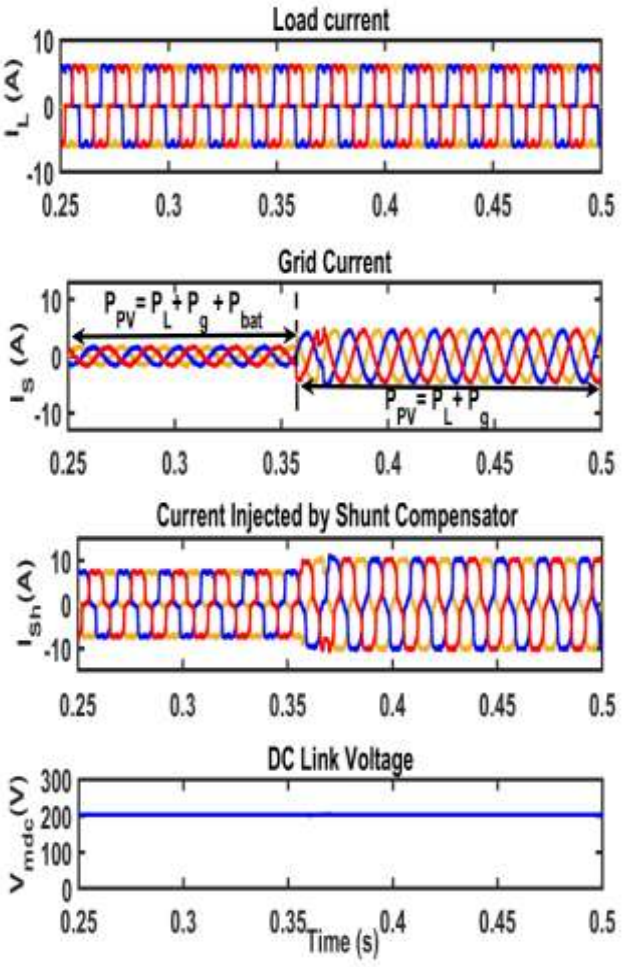


Fig. 6. Nonlinear load current, compensated grid current, shunt current and DC-link voltage.

The source illustrates an SOC-dependent operating transition at t ≈ 0.36 s. Before the transition, PV surplus charges the battery; when the upper SOC threshold is reached, charging is disconnected and the PV surplus is redirected toward the grid. The controller therefore coordinates storage utilization and grid exchange rather than using a fixed battery power request.

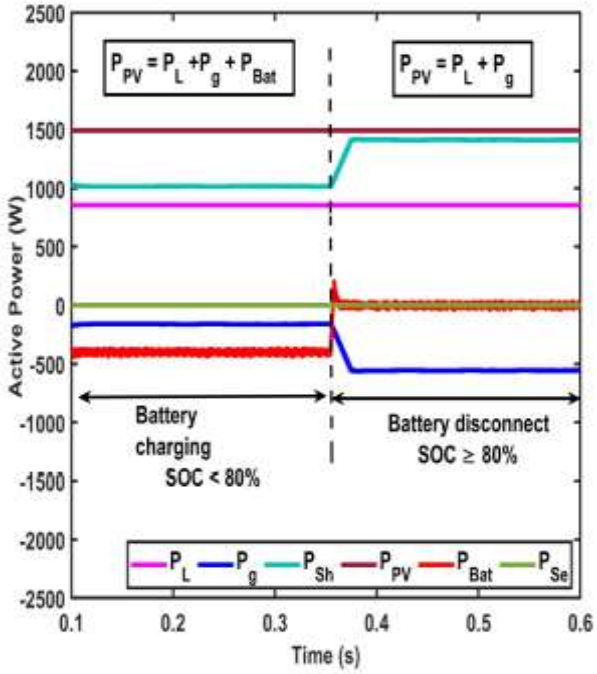


Fig. 7. Source simulation of PV, load, grid, shunt-converter and battery active-power exchange.

VII. DISTURBANCE RESPONSE AND COMPARATIVE DISCUSSION

When the load rises beyond the converter rating at t ≈ 0.25 s, the controller reduces shunt compensation demand and permits the grid to carry additional distorted and reactive current. The source reports 2.46% grid-current THD immediately before the protection event and 7.70% during current limitation; the nonlinear load-current THD in the disturbance case is approximately 27.98%. Thus, the objective changes temporarily from minimum THD to converter survival.

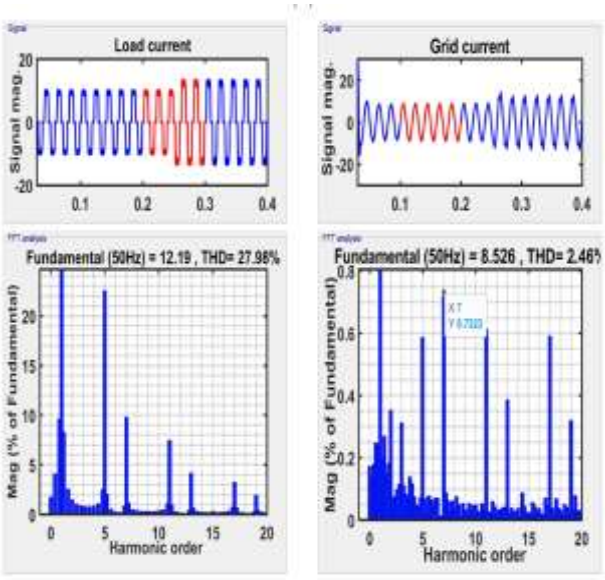


Fig. 8. Harmonic spectra of nonlinear load current and compensated grid current.

The source also examines PV array temperature variation from 25 °C to 45 °C. Battery support improves DC-link transient behavior relative to a PV-only UPQC under the documented test conditions. A separate experimental test uses a 25% grid-voltage sag: the series converter injects the missing voltage and the shunt converter regulates the DC link near 200 V while supplying the corresponding active-power demand.

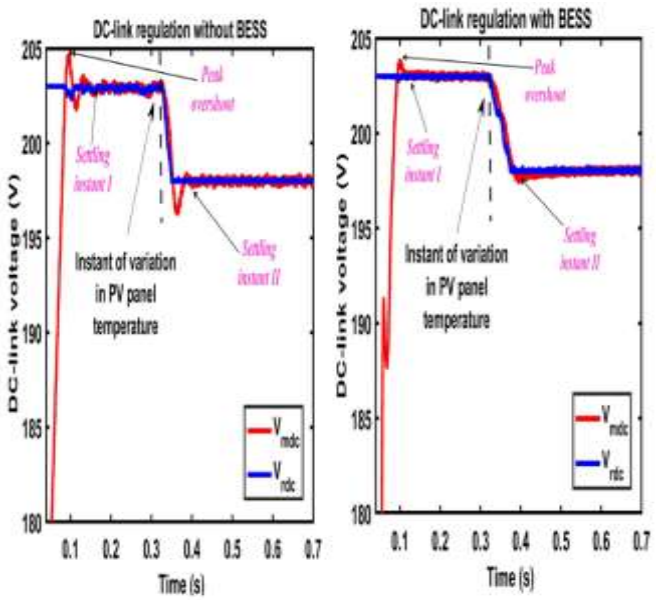


Fig. 9. DC-link response under PV temperature variation, without and with BESS.

The presented figures are reproduced from the uploaded documentation, not generated by a new simulation run. Numerical conclusions are therefore limited to the cases, parameterization and measurements reported in that source.

The major technical contribution is coordinated operation of PV, battery and UPQC using one common DC link, alongside reference-current-based switch protection. This arrangement can reduce grid burden, mitigate harmonic currents and maintain load voltage during sag events. However, the trade-off between temporary grid-current distortion and switch protection needs explicit evaluation against grid-code limits. Reproducibility also requires complete component ratings, switching frequency, sample time, plant parameters and original MATLAB/Simulink files, which are not supplied as executable models in the uploaded document.

In conclusion, the documented PV–BESS–UPQC strategy provides a useful architecture for power-quality improvement and DER management in low-voltage microgrids. Reported tests demonstrate substantial normal-mode harmonic reduction and rapid protective current redistribution during overload. Further work should compare baseline and proposed controls under identical parameter sets, quantify losses and energy efficiency, and independently validate robustness over a wider range of battery SOC and grid disturbances.

REFERENCES

[1] P. Ray, M. L. K. Liyanage, P. K. Ray, and P. S. Puhan, "Grid following and grid forming control modes of der fed vsi with transition of operational modes for microgrid with critical load," in 2023 5th International Conference on Energy, Power and Environment: Towards Flexible Green Energy Technologies (ICEPE), 2023, pp. 1–6.

[2] V. Khadkikar, "Enhancing electric power quality using upqc: A comprehensive overview," IEEE Transactions on Power Electronics, vol. 27, no. 5, pp. 2284–2297, 2012.

[3] A. Heenkenda, A. Elsanabary, M. Seyedmahmoudian, S. Mekhilef, A. Stojcevski, and N. F. A. Aziz, "Unified power quality conditioners based different structural arrangements: A comprehensive review," IEEE Access, vol. 11, pp. 43 435–43 457, 2023.

[4] L. B. G. Campanhol, S. A. O. da Silva, A. A. de Oliveira, and V. D.
Bacon, "Single-stage three-phase grid-tied pv system with universal filtering capability applied to dg systems and ac microgrids," IEEE Transactions on Power Electronics, vol. 32, no. 12, pp. 9131–9142, 2017.

[5] D. Sera, L. Mathe, T. Kerekes, S. V. Spataru, and R. Teodorescu, "On the perturb-and-observe and incremental conductance mppt methods for pv systems," IEEE Journal of Photovoltaics, vol. 3, no. 3, pp. 1070–1078, 2013.

[6] N. Femia, G. Petrone, G. Spagnuolo, and M. Vitelli, "Optimization of perturb and observe maximum power point tracking method," IEEE Transactions on Power Electronics, vol. 20, no. 4, pp. 963–973, 2005.

[7] V. Monteiro, C. Moreira, J. A. Pecas Lopes, C. H. Antunes, G. J. Os´orio, J. P. S. Catal˜ao, and J. L. Afonso, "A novel three-phase multiobjective unified power quality conditioner," IEEE Transactions on Industrial Electronics, vol. 71, no. 1, pp. 59–70, 2024.

[8] S. Devassy and B. Singh, "Performance analysis of solar pv array and battery integrated unified power quality conditioner for microgrid systems," IEEE Transactions on Industrial Electronics, vol. 68, no. 5, pp. 4027–4035, 2021.